

Supplementary Material

Supplementary Material for:

Streamlined digital bioassays with a 3D printed sample changer

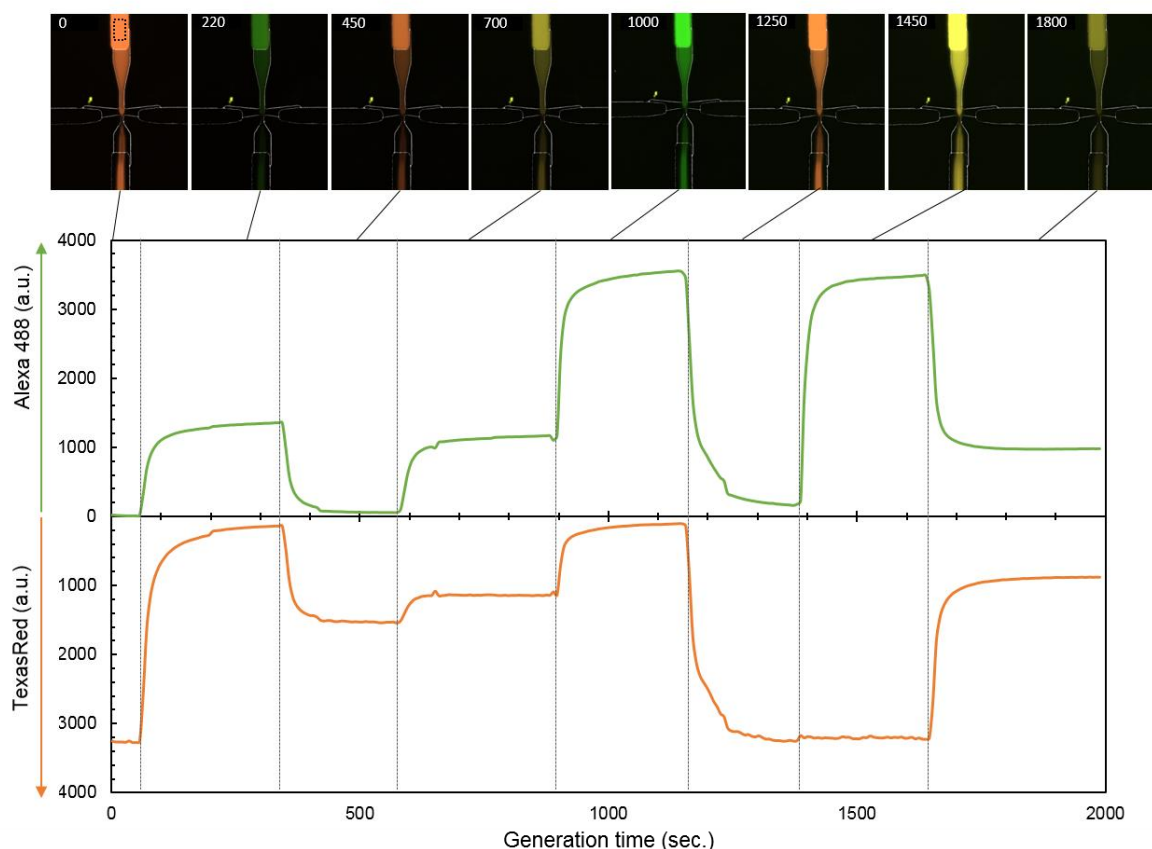


Figure S 1. Time lapse of the droplet generation of 8 barcoded populations using a flow focusing device. From sample 1 to 8 the Alexa488/Texas barcode concentrations in nM are 0/400, 200/0, 0/200, 200/200, 400/0, 0/400, 400/400 and 200/200. The microscopy snapshots correspond a composite image of the chip nozzle (bright field, Texas red and Alexa488 fluorescence channels). The average fluorescence over a portion of the inlet channel (black rectangle in the top left image) is plotted as a function of the generation time.

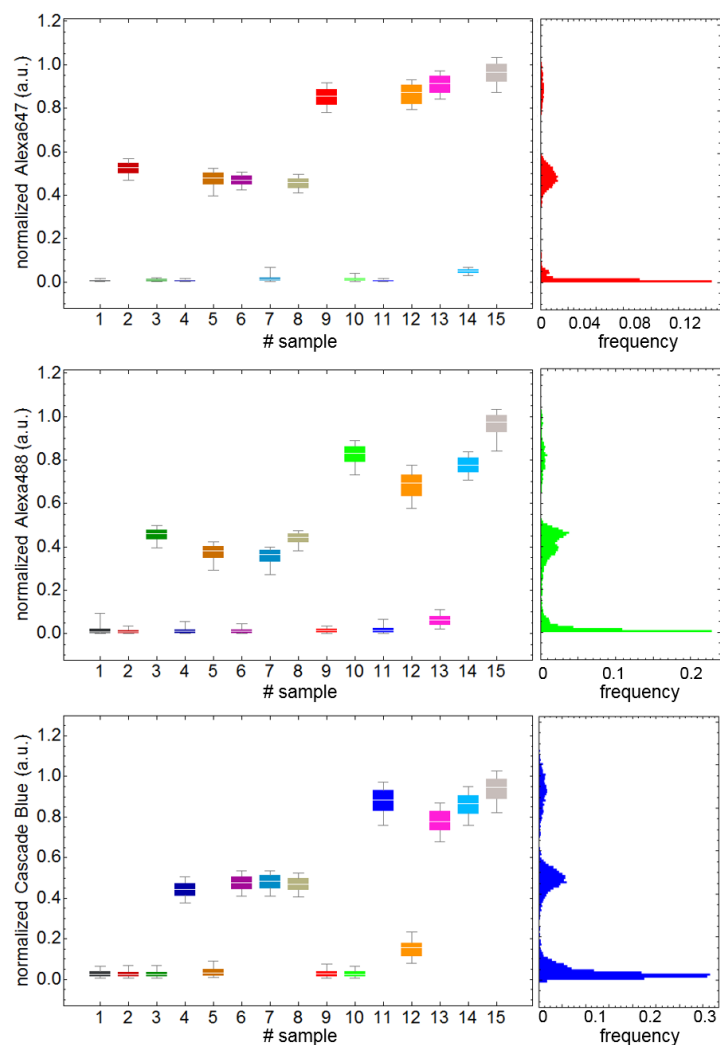


Figure S 2. Extended data from Figure 2. Here, we analyse the fluorescence distribution for the 15 droplet populations in the 3 fluorescence channels (Alexa647, Alexa488 and Cascade Blue). Boxes and whiskers represent the 25-75 % and 10-90% distribution of the droplet fluorescence for each sample. Histograms on the left show the distribution over the full droplet population.

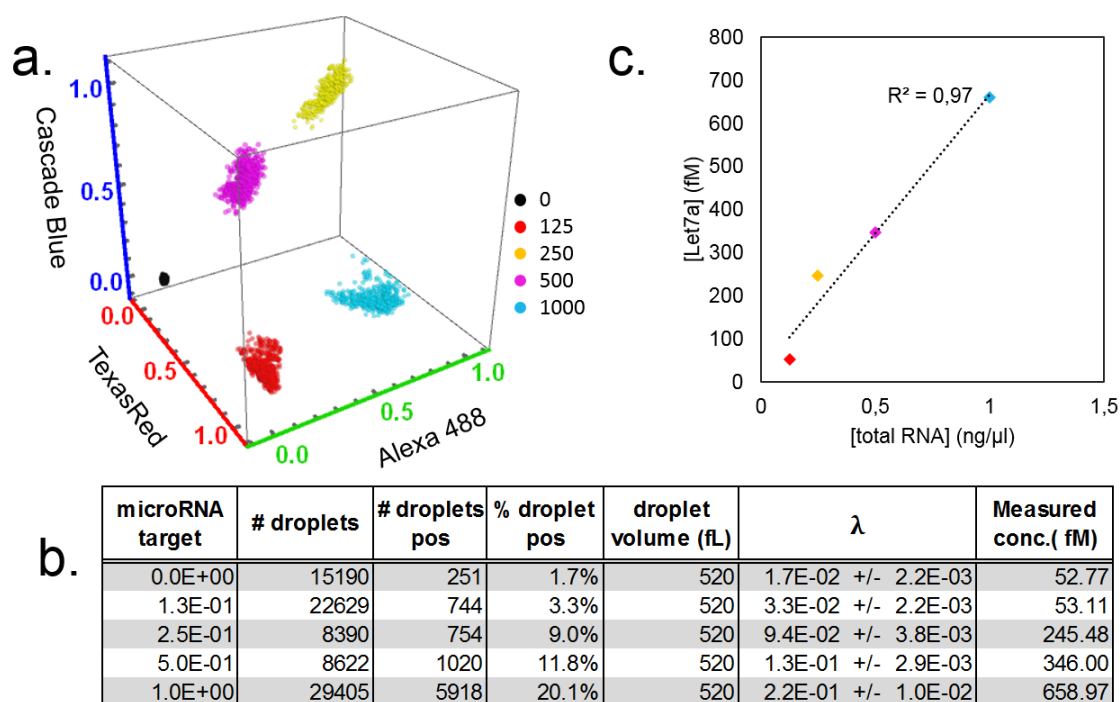


Figure S 3. Detection of Let7a in total RNA extract from human colon tissue. Five barcoded amplification mix containing a varying concentration of total RNA extract are emulsified and Let7a is quantified by a digital readout. **a.** 3D plot of the barcode fluorescence for each droplet population. **b.** Extracted data from the droplet analysis after isothermal incubation. **c.** The measured Let7a concentration (LOB substrated) is plotted against the total RNA extract concentration. The linear correlation demonstrates the proper quantification of the microRNA target in this biological sample.

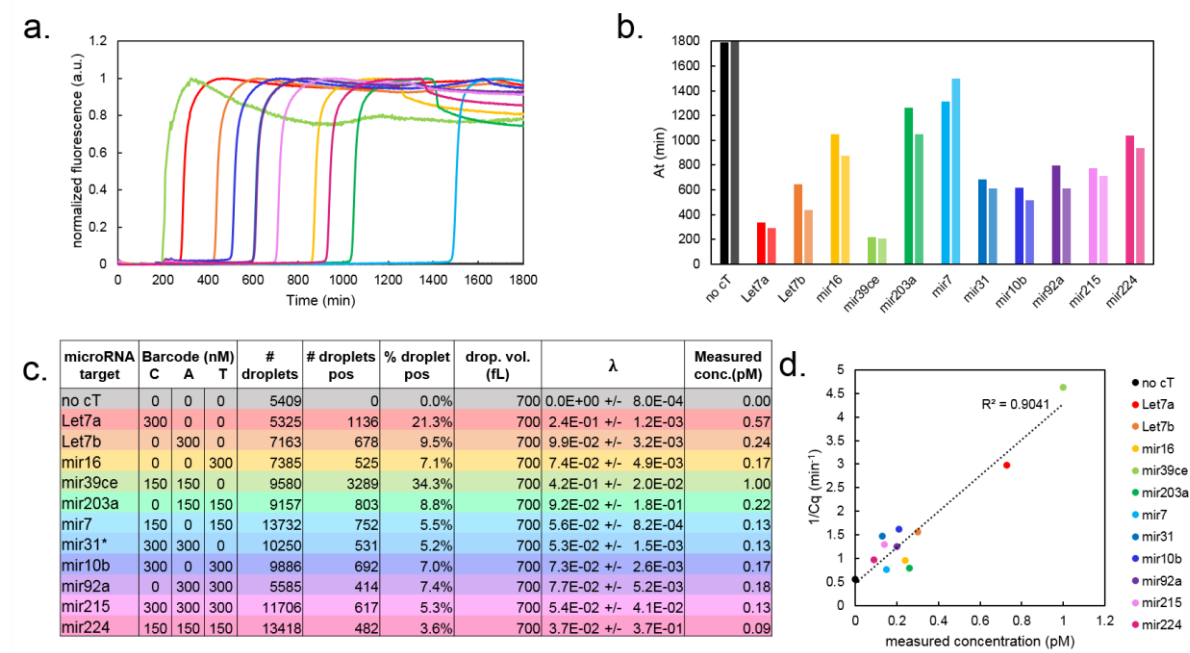


Figure S 4. Extended data from the Figure 4. **a.** Real-time monitoring of the amplification reaction in solution (prior to emulsification). **b.** Extracted amplification time (A_t , corresponding to the time when the fluorescence curves reaches 10 % of the maximum fluorescence). **c.** Extracted data from the droplets analysis after incubation of the emulsion (cf. Supplementary Figure 6 for the analysis procedure). “C”, “A” and “T” denote Cascade Blue, Alexa488 and TexasRed-conjugated dextrans, respectively. **d.** The invert of the A_t is plotted as a function of the measured concentration by droplet digital readout. We observe a linear correlation ($R^2 = 0.90$) that supports the reliability of the digital measurement. Note that a perfect linear correlation is not expected, as the results from the realtime experiment are not standardized (this would require a calibration curve for each microRNA).

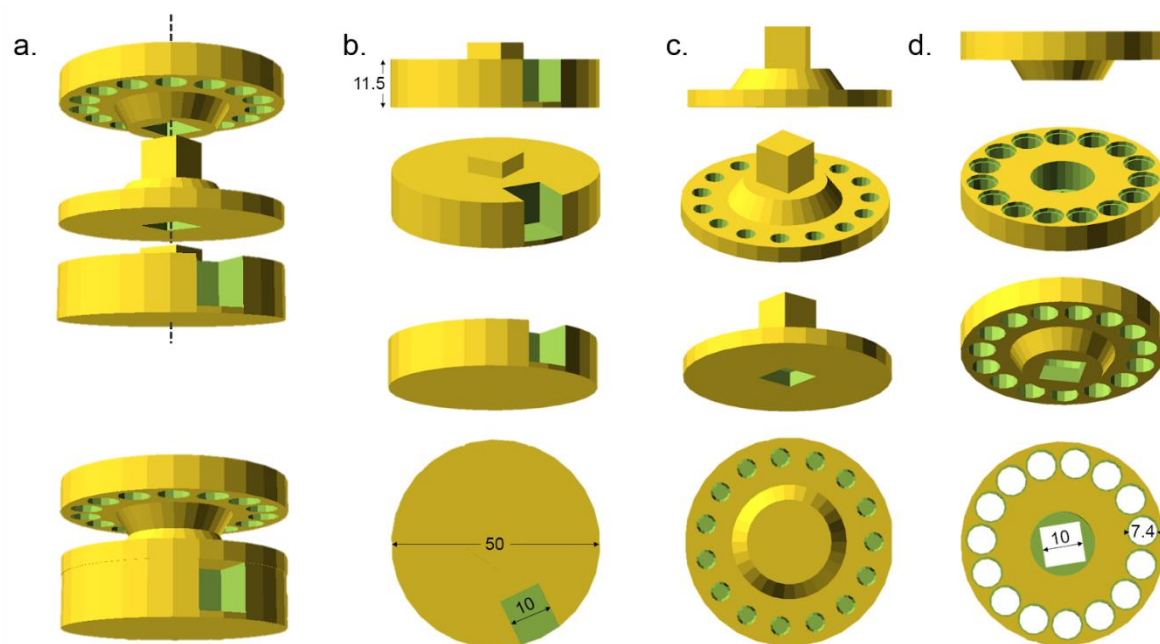


Figure S 5. OpenSCAD design of the 3D printed sample tray. a. The sample tray consists in the assembly of 3 parts. b. Magnet holder (bottom part). b. Middle part. c. Top part. The device was printed using PLA printing filament (30 g = ~2€)

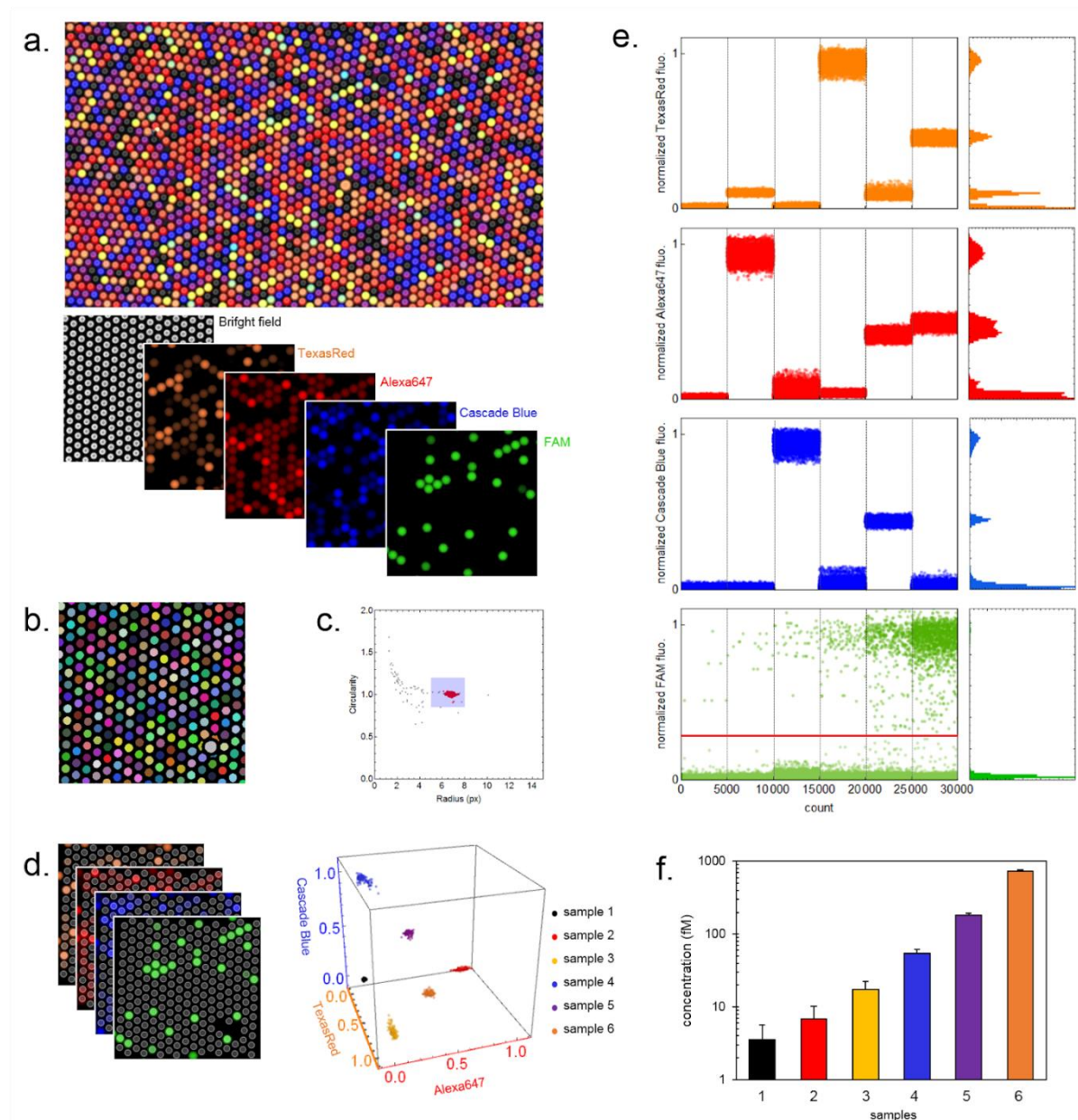


Figure S6. Droplet analysis. The experiment we depict here corresponds to the quantification of the synthetic microRNA Let7a by digital isothermal amplification. From sample 1 to 6, the expected concentration of Let7a is 0, 2.7, 11, 44, 175 and 700 fM respectively. **a.** A monolayer of droplets is imaged by transmission microscopy (bright field) and epifluorescence microscopy (including here the 3 channels for the barcodes TexasRed, Alexa647 and Cascade Blue and the channel corresponding to the fluorescent output of the digital readout, FAM). **b.** The bright field image is used to segment individual droplets. **c.** The droplets are selected on the basis of their size (radius in pixel) and circularity (> 0.9). The blue box includes all droplets that fit the size and circularity parameters. An additional density filter, excluding the few droplets that are isolated in this box, is applied and the object represented in red is kept for the downstream analysis. **d.** 3D plot of the droplets fluorescence barcodes : for each selected droplet, the fluorescence in each channel is averaged over a disk of center corresponding to the object centroid and radius r (r being slightly smaller than the droplet radius). The droplets population are sorted according to their fluorescence in the barcode's channels. **e.** Fluorescence plots of the barcodes and probe fluorescence after sorting. **f.** The concentration of the target molecule (here, Let7a) is calculated using the Poisson law, assuming a random distribution of the targets across the droplets

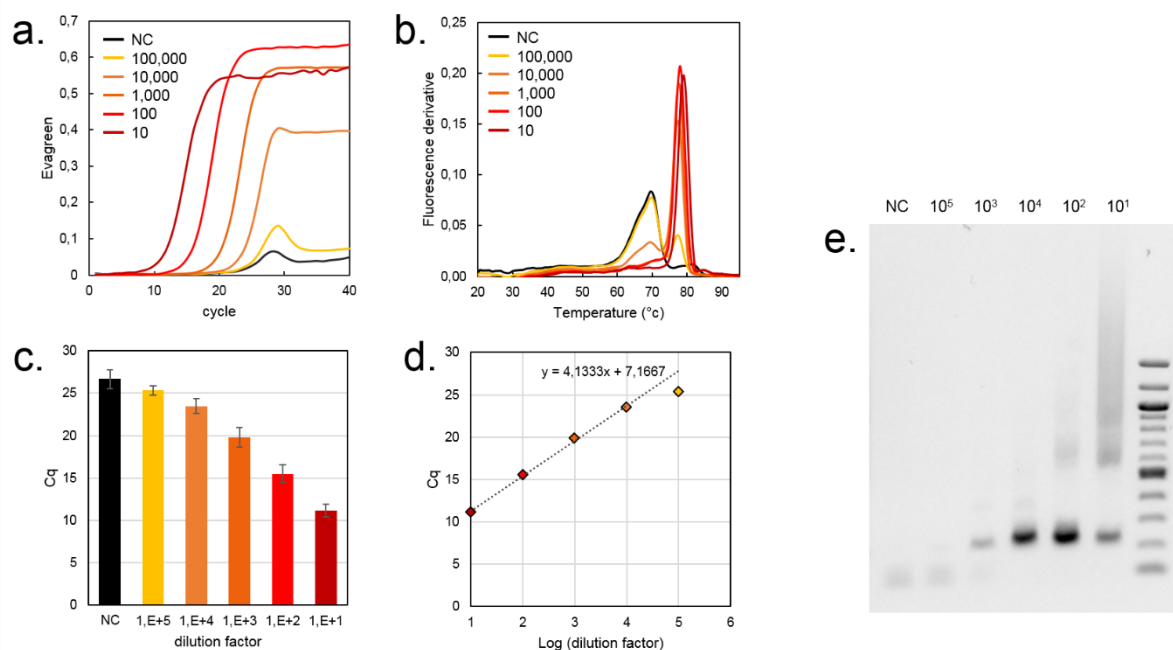


Figure S 7. Real-time PCR. Real-time PCR of the 163 bases long amplicon starting with various template dilutions ranging from a 10^1 to a 10^5 -dilution factor. **a.** Real-time monitoring of the qPCR amplification in solution by Evagreen fluorescence signal recording. **b.** Corresponding melt curves. **c.** Extracted cycle quantification (Cq) values from the real-time curve analysis. **d.** Cq values are plotted as a function of the used dilution factor. We observe a linear correlation ($R^2 = 0.998$) similar to the one observed in Figure 6 with ddPCR. **e.** Amplicon migration in an 0.8 % w/v agarose gel.

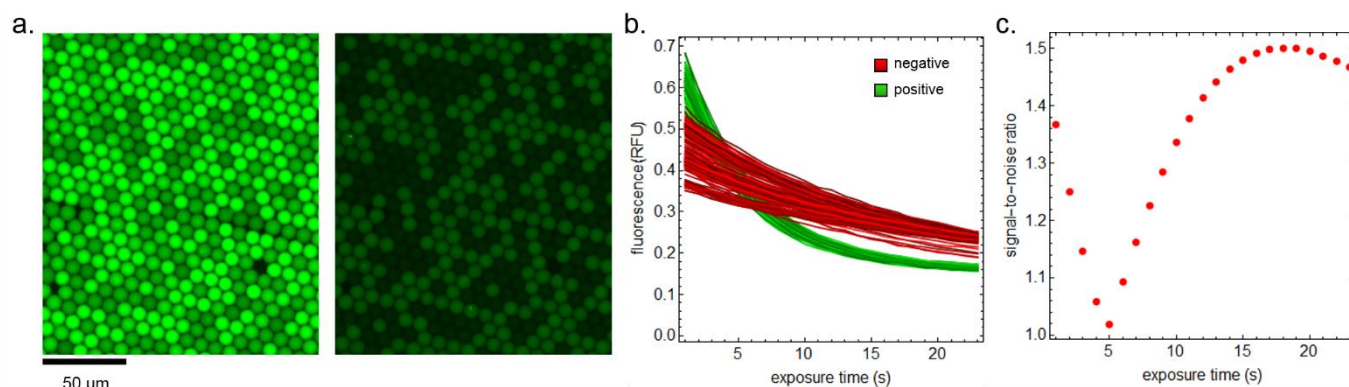


Figure S 8. Inverted contrast following photobleaching of droplets after digital PCR. **a.** Microscopy images of a 2D droplet array after an exposure time of $t = 1$ s (left) and $t = 20$ s (right). The acquisition time is 1 s. After PCR amplification, we noticed that Evagreen fluorescence is more resistant to photobleaching in negative droplets than in positive droplets. As a result, the positive droplets become less fluorescent than the negative droplet, contrary to classical droplet digital PCR readout. **b.** Fluorescence emission of the droplets as a function of the exposure time (red time traces = negative droplets, green time traces = positive droplets). **c.** Signal-to-noise ratio (SNR) as a function of the exposure time (SNR = 1.37 at $t = 1$ s and 1.47 at $t = 20$ s).

Table S 1. Nucleic acid sequences used throughout the study. "*" denotes phosphorothioate backbone modification. "p" denotes 3'-phosphate modification. Upper and lower cases represent 2'-deoxyribonucleotide and ribonucleotide, respectively. BHQ2 stands for Black Hole Quencher 2 and is used as a quencher of the Atto633 fluorophore.

| ID | Sequence | function |
|---|---|----------------|
| Isothermal amplification for the digital detection of microRNA | | |
| α | CATTCTGGACTG | |
| $\alpha\text{to}\alpha$ | C*A*G*T*CCAGAATGCAGTCCAGAAp | aT |
| pT α | T*T*T*T*TCAGTCCAGAATGp | pT |
| rT α | Atto633 *A*T*TCTGAATGCAGTCCAGAAT BHQ2 | rT |
| Let7a $\text{to}\alpha$ | TGCAGTCCAGAAAGTTTGACTCAAACCTATAACAACCTACTACCTCAp | cT |
| Let7b $\text{to}\alpha$ | TG-CAGTCCAGAA-GTTTGACT-CAAACCACACAACCTACTACCTCA | cT |
| 16 $\text{to}\alpha$ | TG-CAGTCCAGAA-GTTTGACTC-A-CGCCAAUUAUUUACGTGCUGCUA | cT |
| 39 $\text{to}\alpha$ | TG-CAGTCCAGAA-GTTTGACTC-A-CAAGCTGATTTACACCC | cT |
| 203a $\text{to}\alpha$ | TG-CAGTCCAGAA-GTTTGACTCAA-CTAGTGGTCCTAAACATTTAC | cT |
| 7 $\text{to}\alpha$ | TGCAGTCCAGAA-GTTTGACTCA-AACAACAAAATCACTAGTCTTCCA | cT |
| 31 $\text{to}\alpha$ | TG-CAGTCCAGAA-GTTTGACTC-A-GATGGCAATATGTTGGCA | cT |
| 10b $\text{to}\alpha$ | TGCAGTCCAGAA-GTTTGACTCA-CACAAATTCGGTTCTACAGGGTA | cT |
| 92a $\text{to}\alpha$ | TG-CAGTCCAGAA-GTTTGACTCAAGCATTGCAACCGATCCCAACC | cT |
| 215 $\text{to}\alpha$ | TG-CAGTCCAGAA-GTTTGACTCA-GTCTGTCAATTCATAGGTCAT | cT |
| 124 $\text{to}\alpha$ | TG-CAGTCCAGAA-GTTTGACTCA-GGCATTACCCGCGTGCCTT | cT |
| Let7a-5p | ugagguaguagguuguauaguu | microRNA |
| Let7b-5p | ugagguaguagguugugugguu | microRNA |
| miR-16-5p | uagcagcacguaaaauuugcg | microRNA |
| cel-miR39-5p | ucaccggguguaaaucagcuug | microRNA |
| miR-203a-3p | gugaaauguuuaggaccacuag | microRNA |
| miR-7-5p | uggaagacuagugauuuuguuguu | microRNA |
| miR-31- | ugcuauGCCAACAUauGCCauc | microRNA |
| miR-10b-5p | uaccuuguagaaccgaauuugug | microRNA |
| miR-92a-5p | agguugggaucgguugcaaugcu | microRNA |
| miR215-5p | augaccuauGAAUUGACAGAC | microRNA |
| miR124-3p | aaggcacgCGGUGAAUGCC | microRNA |
| Droplet digital PCR | | |
| fw primer | CCATGCTAAGGAATTACAG | forward primer |
| rv primer | ATTTTATTTGCAATGAAGCG | reverse primer |